Wind and Structures, Vol. 14, No. 3 (2011) 239-252
DOI: http://dx.doi.org/10.12989/was.2011.14.3.239

Wind-induced responses of Beijing National Stadium

YANG Q.S.* and TIAN Y.J.

School of Civil Engineering, Beijing Jiaotong University, Beijing 100044

(Received July 21, 2009, Accepted December 8, 2010)

Abstract. The wind-induced mean, background and resonant responses of Beijing National Stadium are investigated in this paper. Based on the concepts of potential and kinetic energies, the mode participation factors for the background and the resonant components are presented and the dominant modes are identified. The coupling effect between different modes of the resonant response and the coupling effect between the background and resonant responses are analyzed. The coupling effects between the background and resonant components and between different modes are found all negligible. The mean response is approximately analogous to the peak responses induced by the fluctuating wind. The background responses are significant in the fluctuating responses and it is much larger than the resonant responses at the measurement locations.

Keywords: background response; resonant response; mode participation coefficient; coupling effect; mode participation factor; stadium.

1. Introduction

The Beijing National Stadium (BJNS, Fig. 1) is the main stadium for the opening and closure ceremony of the Beijing 2008 Olympic Games. It is located at the center of Beijing Olympic Park in the northern part of the Beijing City, China. The park is approximately 8 km north of the Forbidden City. The form and appearance of BJNS looks like a nest of birds and is popularly

Fig. 1 Beijing National Stadium

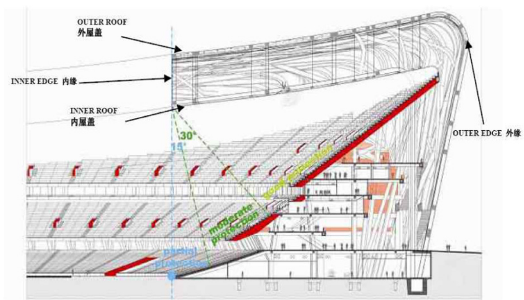

Fig. 2 Profile of BJNS roof

* Corresponding Author, Professor, E-mail: qshyang@bjtu.edu.cn

named as the Bird Nest.

The saddle-shaped roof of BJNS, with a 332.3 × 296.4 m elliptical plan, consists of steel skeleton with skins of the translucent Ethylene Tetra Fluoro Ethylene (ETFE) membrane panels on the outer roof and edge, and the Poly Tetra Fluoro Ethylene (PTFE) membrane panels on the inner roof and edge (Fig 2). A 185.3 m × 127.5 m elliptical opening is located at the roof center. The stadium facades are fully opened with an open concourse. The wind-induced response behaviour of the BJNS has been properly analyzed for sufficient safety.

To determine the wind load on BJNS, a 1:300 scaled structure model was tested in a wind tunnel with 509 pressure taps installed over the outer and inner roofs. Sets of measured data under wind load excitation from 36 wind directions at equally spaced 10-degree intervals in the polar coordinates were recorded. Maps of the wind pressures on both the inside and outside surfaces of the outer and inner roofs for direction θ=20° are presented in Fig.3 as an example of these measurements.

All wind loads with 100-year return period were determined in accordance with the Chinese Load Code (GB50009-2001), which is based on a 10-minute mean wind speed at 10m height above ground in open country and adjusted in accordance with the site conditions to take into account the upwind terrain roughness.

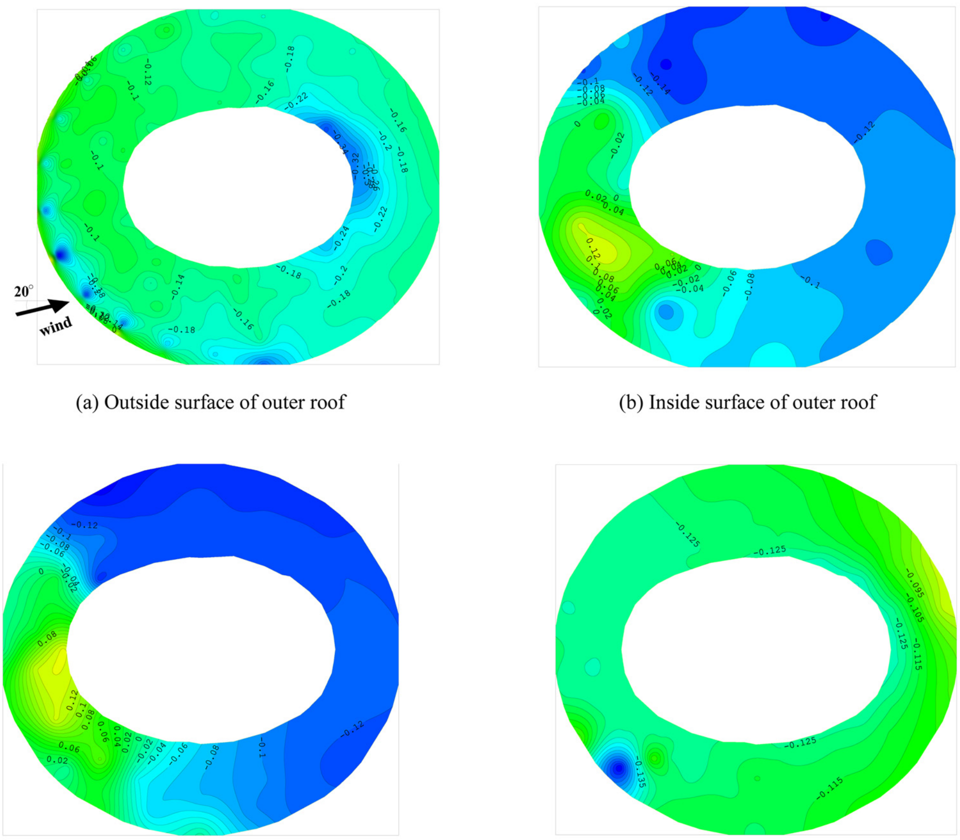

(a) Outside surface of outer roof

(b) Inside surface of outer roof

(c) Inside surface of inner roof

(d) Outside surface of inner roof

Fig. 3 Maps of the wind pressures (kN/m^2)

2. General procedures

The equation of motion of the structure can be written as

$$\boldsymbol{M}\ddot{\boldsymbol{X}}(t) + \boldsymbol{C}\dot{\boldsymbol{X}}(t) + \boldsymbol{K}\boldsymbol{X}(t) = \boldsymbol{L}\boldsymbol{P}(t) \tag{1}$$

where ***M, C, K*** are the mass, damping and stiffness matrices, respectively; $\boldsymbol{P}(t)$ is the measured fluctuation wind load vector; $X(t), \dot{X}(t), \ddot{X}(t)$ denote the displacement, velocity and acceleration response vectors, respectively; L is the index matrix of the load vector. Eq.(1) can be rewritten in the generalized coordinates to become

$$\ddot{\boldsymbol{Q}}(t) + D\dot{\boldsymbol{Q}}(t) + \Omega^2\boldsymbol{Q}(t) = \Phi^T\boldsymbol{L}\boldsymbol{P}(t) \tag{2}$$

where

$$\mathrm{X}(t) = \Omega\mathrm{Q}(t) \tag{3}$$

and $\boldsymbol{Q}(t), \dot{\boldsymbol{Q}}(t), \ddot{\boldsymbol{Q}}(t)$ are the generalized displacement, velocity and acceleration response vectors, respectively; $\Phi = [\varphi_1, \varphi_2 \ldots\ldots \varphi_N]$ is the modal matrix; $\Omega = diag[\omega_1\ \omega_2 \ldots\ldots \omega_N]$ is a diagonal matrix of the circular frequencies ω_j; $\boldsymbol{D} = diag[2\zeta_1\omega_1\ 2\zeta_2\omega_2\ \ldots\ldots\ 2\zeta_N\omega_N]$ is the decoupled damping matrix, and ζ_j is the damping ratio of the jth mode.

In the generalized displacement response vector$\mathrm{Q}_{(t)}$, each time history can be assumed to be the summation of the background component with lower frequencies and the resonant component with higher frequencies (Davenport 1995) as shown in Fig. 4. Therefore the structural displacement vector can also be considered as the summation of background component and the resonant component responses with

$$\boldsymbol{X}(t) = \boldsymbol{X}_b(t) + \boldsymbol{X}_r(t) = \Phi\boldsymbol{Q}_b(t) + \Phi\boldsymbol{Q}_r(t) \tag{4}$$

where $\mathrm{X}_b(t)$, $\mathrm{X}_r(t)$ represent the time history of the background component and resonant component of the structural responses; and $\boldsymbol{Q}_b(t) = [q_{1,b}(t)\ q_{2,b}(t) \ldots q_{N,b}(t)]^T$, $\boldsymbol{Q}_r(t) = [q_{1,r}(t)\ q_{2,r}(t) \ldots q_{N,r}(t)]^T$.

The structural response of any DOF, says the mth, can be written as follows (Tian 2009)

$$\sigma_m^{\ 2} = \sum_{j=1}^{N}\sum_{k=1}^{N} \sigma_{mj}\sigma_{mk,\mathrm{b}}\sigma_{j,\mathrm{b}}\sigma_{k,\mathrm{b}} + 2\sum_{j=1}^{N}\sum_{k=1}^{N} \varphi_{mj}\varphi_{mk}\beta_{jk,\mathrm{br}}\sigma_{j,\mathrm{b}}\sigma_{k,\mathrm{r}} + \sum_{j=1}^{N}\sum_{k=1}^{N} \varphi_{mj}\varphi_{mk}\gamma_{jk,\mathrm{r}}\sigma_{j,\mathrm{r}}\sigma_{k,\mathrm{r}} \tag{5}$$

It is shown the response depends on the variance of the responses of each mode. In Eq. (5), φ_{mj} and φ_{mk} are the *j*th-mode and the *k*th-mode shape displacements, respectively; $\sigma_{\mathrm{j,b}}$ and $\sigma_{\mathrm{j,r}}$ are the jth-mode background and resonant responses, respectively; $\sigma_{\mathrm{k,b}}$ and $\sigma_{\mathrm{k,r}}$ are the kth-mode background and resonant responses, respectively; $\beta_{\mathrm{jk,br}}$ is the component coupling factor between the jth-mode background response and the *k*th-mode resonant response; and $\gamma_{jk,\mathrm{b}}$ and $\gamma_{jk,\mathrm{r}}$ are the mode coupling factors between the *j*th-mode and *k*th-mode background response and between the *j*th-mode and *k*th-mode resonant response, respectively. These items are calculated as follows.

The variance of *j*th-mode background response is obtained by neglecting the inertial item and the

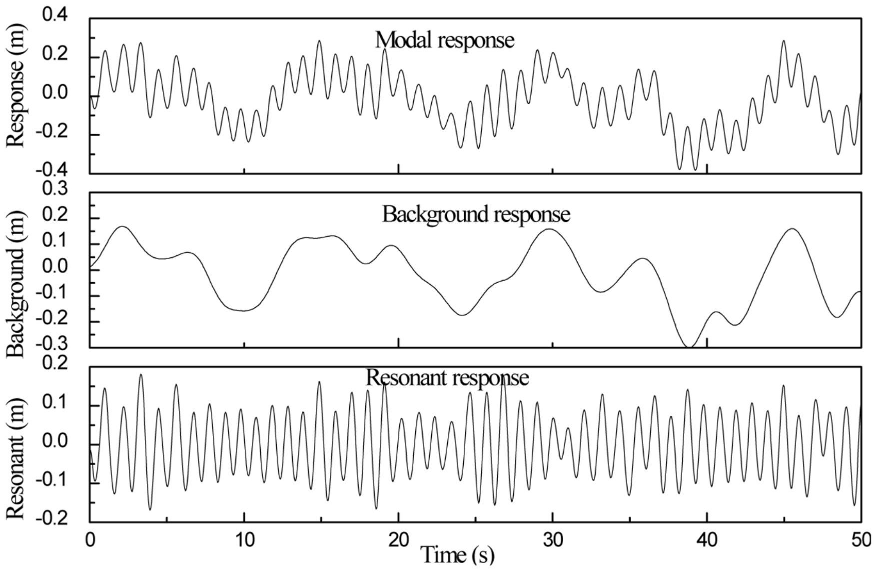

Fig. 4 Background and resonant response

damping item in the equation of motion of the jth-mode with (Tian 2007a)

$$\sigma_{j,\mathrm{b}}^2 = H_{j,\mathrm{b}}^2 \varphi_j^T \boldsymbol{L} \cdot \int_{-\infty}^{+\infty} \boldsymbol{S_{pp}}(\omega)\mathrm{d}w \cdot \boldsymbol{L^T} \varphi_j \tag{6}$$

in which $S_{pp}(\omega)$ is the cross-power spectrum density of the measured wind pressures; and $H_{j,b}$ is referred to as the transfer function of the background component with $H_{j,b}=1/\omega_j^2$. The time history of the resonant component can therefore be obtained as

$$q_{j,\mathrm{r}}(t) = q_j(t) - q_{j,\mathrm{b}}(t) \tag{7}$$

and the variance of the resonant component is defined as

$$\sigma_{j,\mathrm{r}}^2 = \int_{-\infty}^{+\infty} H_{j,\mathrm{r}}(\omega)\varphi_j^T \boldsymbol{L}\boldsymbol{S}_{pp}(\omega)\boldsymbol{L^T}\varphi_j H^*{}_{j,\mathrm{r}}(\omega)\mathrm{d}\omega \tag{8}$$

where $\boldsymbol{H}_{j,\mathrm{r}}(\omega)$ and $\boldsymbol{H^*}_{j,\mathrm{r}}(\omega)$ denote the transfer function and its conjugate of the resonant response of the jth-mode and it can be calculated as

$$H_{j,\mathrm{r}}(\omega) = \frac{1}{\omega_j^2}\left(\frac{1}{1-\omega^2/\omega_j^2 + i\cdot 2\zeta_j\omega/\omega_j} - 1\right) \tag{9}$$

The expressions of the coupling factors in Eq.(5) have been given in Tian(2009) and the following is the brief introduction of these expressions. The component coupling factor, $\beta_{jk,\mathrm{br}}$, between the jth-mode background response and the kth-mode resonant response can be written as

$$\beta_{jk,\mathrm{br}} = \frac{\mathrm{Re}\left[\int_{-\infty}^{+\infty} H_{j,\mathrm{b}}\varphi_j^T \boldsymbol{L}\boldsymbol{S}_{pp}(\omega)\boldsymbol{L^T}\varphi_k H^*{}_{k,\mathrm{r}}(\omega)\mathrm{d}\omega\right]}{\sigma_{j,\mathrm{b}}\sigma_{k,\mathrm{r}}} \tag{10}$$

where Re(•) means the real part of a complex value. The mode coupling factor $\gamma_{jk,r}$ between the jth-mode and the kth-mode resonant responses are defined as

$$\gamma_{jk,r} = \frac{\mathrm{Re}\left[\int_{-\infty}^{+\infty} H_{j,\mathrm{r}}(\omega)\varphi_j^T \boldsymbol{L}\boldsymbol{S}_{pp}(\omega)\boldsymbol{L}^{\mathrm{T}}\varphi_k H^*_{k,\mathrm{r}}(\omega)\mathrm{d}\omega\right]}{\sigma_{j,\mathrm{r}}\sigma_{k,\mathrm{r}}} \tag{11}$$

while the mode coupling factor $\gamma_{jk,\mathrm{b}}$ between the jth-mode and the kth-mode background responses are expressed as,

$$\gamma_{jk,b} = \frac{\int_{-\infty}^{+\infty} H_{j,\mathrm{b}}\varphi_j^T \boldsymbol{L}\boldsymbol{S}_{pp}(\omega)\boldsymbol{L}^{\mathrm{T}}\varphi_k \boldsymbol{H}_{k,\mathrm{b}}\mathrm{d}\omega}{\sigma_{j,b}\sigma_{k,b}} \tag{12}$$

where $H_{k,\mathrm{b}}= 1/\omega_j^2$ and $H_{j,\mathrm{b}}= 1/\omega_k^2$ are constants, and their correlation always equals to unity.

It can be seen from Eqs.(5) - (12) and that the contribution of a vibration mode to the structural response depends on the mode order, the correlation between the mode shape and the spatial distribution of wind load, and the difference between the dominant frequency of wind load and the natural frequency of the structure; i.e., the lower the mode order, the larger the correlation between the mode shape and the spatial distribution of wind load, the smaller the difference between the dominant frequency of wind load and the natural frequency of the structure, the larger would be the structural response. Satisfactory solution may be achieved by considering a few lower modes only if the shapes of the lower vibration modes are highly consistent to the spatial distribution of the wind load. For example, the response of a high-rise building or a super-high structure excited by wind load can be obtained with great accuracy based on the first three modes. While, if the mode shapes have little correlation to the spatial distribution of wind loads, the responses are influenced by multiple modes or they are associated with structural modes of the higher frequencies. Hence, the natural vibration modes and frequencies of the BJNS are analyzed first and they are shown in Figs. 5 and 6.

It is shown that the natural frequencies are spaced closely (Fig. 5), and the mode shapes are

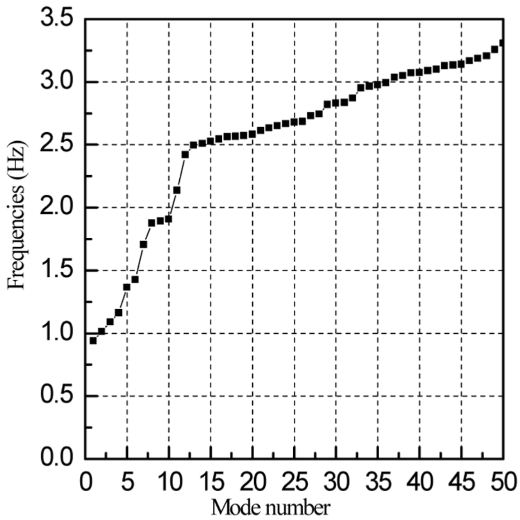

Fig. 5 Distribution of frequencies

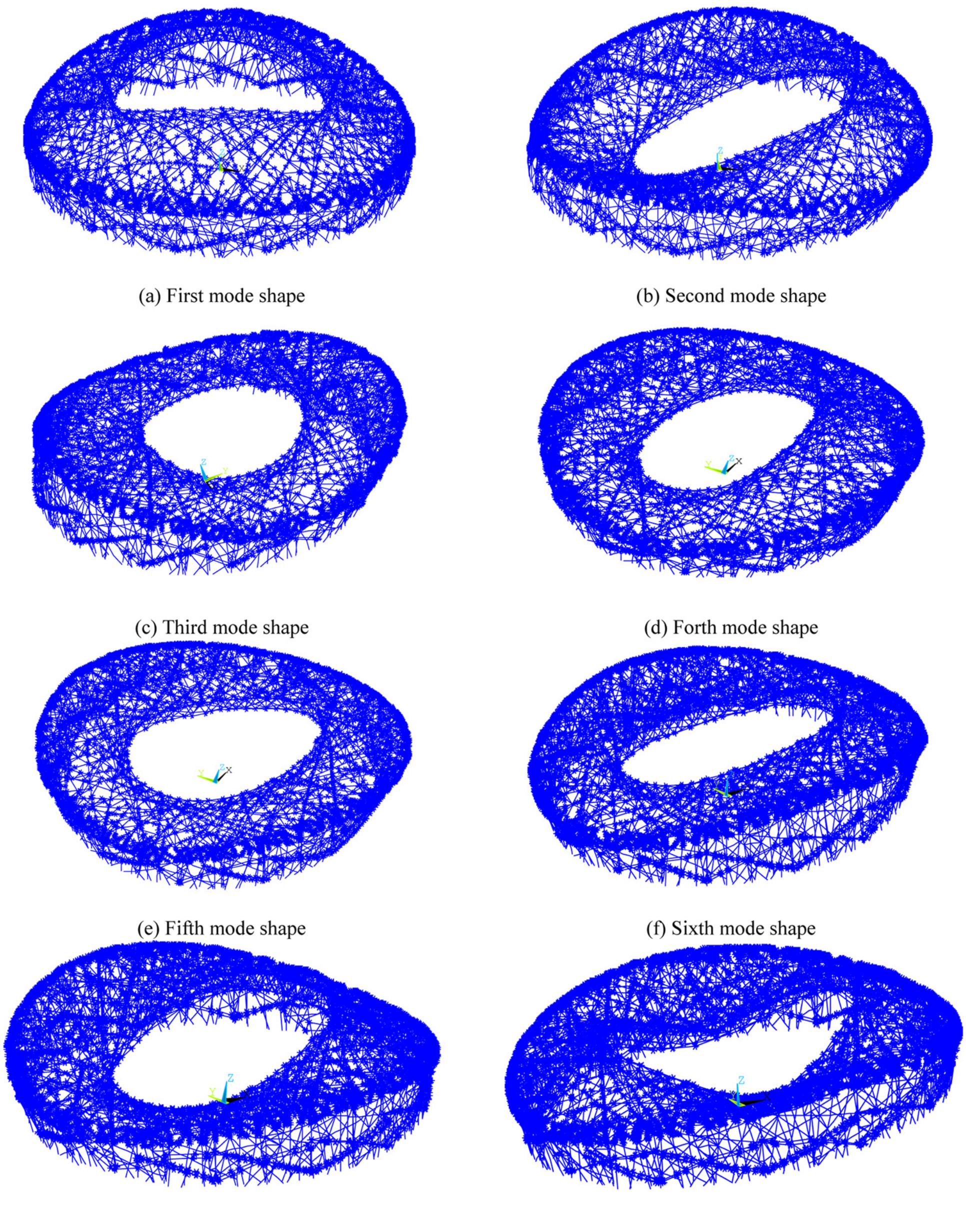

(a) First mode shape (b) Second mode shape

(c) Third mode shape (d) Forth mode shape

(e) Fifth mode shape (f) Sixth mode shape

(g) Seventh mode shape (h) Eighth mode shape

Fig. 6 First eight mode shapes of BJNS

complex (Fig. 6), and are not very consistent with the distribution of wind loads on the roofs (Fig. 3). Therefore, multiple modes should be taken into account, and some higher order modes may be more significant than the lower ones. If all of the modes are considered, the response analysis of a long span structure, such as the BJNS, will be a time-consuming task, and it is necessary to find a way to extract the dominant modes, i.e., the ones contributing greatly to the structural responses, on the basis of achieving a satisfied precision with these selected dominant modes. Section 3 will focus on the dominant mode selection by defining the mode participation factors of the background component and the resonant component.

Section 4 will identify the dominant modes of BJNS and the background and resonant responses are analyzed respectively while the coupling effects of both the background responses and resonant responses are investigated. The fluctuating wind responses result from the background and the resonant responses while the coupling item between the two components are examined. The mean, background and resonant components are then combined to obtain the maximum and minimum responses. Finally, Section 5 gives the characteristics of the wind-induced responses of roof of the BJNS.

3. Dominant modes

A common procedure to extract the dominant modes is by generating the Load-Dependent Ritz Vectors (Wilson 1982, Nour-Omid 1985 and Gu 2000). Since the spatial distributions of wind loads are much very complex, the Proper Orthogonal Decomposition is explored to decompose the wind field into a product of spatial distributions and a random field (Wu 2007). A Ritz vector contributes significantly to the total responses without knowledge of its contributions to the background responses and the resonant responses. Additionally, some spatial distributions are discarded since their energies are very small while the structural responses excited by these spatial distributions may not be small. To overcome these drawbacks, a procedure to identify respectively the dominant modes for the background component and the resonant component is presented in this section.

Since the background response of a mode is not dependent on the ratio of frequency of the wind load excitations to the natural frequency of the structure, the time history of the background response is a quasi-static process in nature. Hence the internal energy of the structure includes only the strain energy or the potential energy. It gives a clue to extract the dominant modes of the background responses based on the strain energy. This section gives the mode energy participation coefficient of the background response, which is the ratio of mode strain energy to the total strain energy induced by the background responses. This coefficient may be used to extract the dominant modes of the background responses.

In fact, the resonant response of a mode is a vibration process, and it contains both the mode strain energy and the kinetic energy. Thus the mode energy participation coefficient of the resonant response is the ratio of the summation of the mode strain energy and the kinetic energy for a mode to the corresponding energy contained in the structure.

3.1 Mode energy participation factors for background responses

The time histories of the background displacements can be regarded as the quasi-static processes. The work done by the fluctuating wind forces when they undergo the background displacements can be transformed into the strain energy or potential energy, that is (Tian, 2007a; 2007b),

$$W_{\mathrm{b}} = \frac{1}{2}\mathbf{X}_{\mathrm{b}}^{\mathrm{T}}(t)\mathbf{LP}(t) = \frac{1}{2}\sum diag[\mathbf{LP}(t)\mathbf{X}_{\mathrm{b}}^{\mathrm{T}}(t)] = \frac{1}{2}\sum diag[\mathbf{LP}(t)\mathbf{P}^{T}(t)\mathbf{L}^{T}\mathbf{K}^{-1}] \tag{13}$$

where $X_b(t)$ is time history of background displacement vector; $\sum diag[\bullet]$ denotes the summation of diagonal elements of matrix $[\bullet]$.

The expectation or mean value of the work down $\boldsymbol{W_b}$ is

$$W_{\mathrm{b,m}} = \frac{1}{2}\sum diag[\mathbf{L}\cdot \mathrm{E}[\mathbf{P}(t)\mathbf{P}^T(t)]\cdot \mathbf{L}^T\mathbf{K}^{-1}] = \frac{1}{2}\sum diag\left[\mathbf{L}\cdot \int_{-\infty}^{+\infty}\mathbf{S}_{pp}(\omega)dw\cdot \mathbf{L}^T\mathbf{K}^{-1}\right] \quad (14)$$

The time history of background displacement response of the jth mode is calculated as follows

$$q_{j,\mathrm{b}}(t) = H_{j,\mathrm{b}}\varphi_j^T\boldsymbol{LP}(t) \quad where \quad H_{j,\mathrm{b}} = 1/w_j^2 \quad (15)$$

and its contribution to the total background responses is

$$\mathrm{X}_{j,\mathrm{b}}(t) = \varphi_j q_{j,\mathrm{b}}(t) = \varphi_j H_{j,b}\varphi_j^T\mathbf{LP}(t) \quad (16)$$

The work done by the fluctuating winds when they undergo the background displacement of the jth mode is

$$W_{j,\mathrm{b}} = \frac{1}{2}\mathbf{X}_{j,\mathrm{b}}^T(t)\mathbf{LP}(t) = \frac{1}{2}\sum diag[\mathbf{LP}(t)\mathbf{X}_{j,\mathrm{b}}^{\mathrm{T}}(t)] = \frac{1}{2}\sum diag[\mathbf{LP}(t)\mathbf{P}^T(t)\mathbf{L}^T\varphi_j H_{j,b}\varphi_j^T] \quad (17)$$

The expectation of the work down $W_{\mathrm{j,b}}$ is

$$W_{j,\mathrm{b,m}} = \frac{1}{2}\sum diag\left[\mathbf{L}\cdot \int_{-\infty}^{+\infty}\mathbf{S}_{\mathrm{pp}}(\omega)dw\cdot \mathbf{L}^T\varphi_j H_{j,b}\varphi_j^T\right] \quad (18)$$

The jth mode energy participation coefficient of the background response is defined as follows

$$\lambda_{j,\mathrm{b}} = \frac{W_{j,\mathrm{b},m}}{W_{\mathrm{b,m}}} \quad (19)$$

The mode energy participation coefficient of background response represents the mean contribution ratio of the mode displacement of background response to the total displacement of background response. The participation factors of the selected modes are calculated and sorted in descending order and they are added together. Both the precision of the displacement of background response and the number of selected modes are controlled by a predefined minimum value of the mode participation factors and the cumulative factors. The predefined minimum value of the cumulative factors for this study is 95%.

3.2 Mode energy participation factors for resonant responses

When resonant vibration occurs, the work done by the external forces equals to the summation of the kinetic energy and the potential energy. The kinetic energy and the potential energy are related respectively to the velocity and the displacement. Hence the work done by the fluctuating wind loads when they undergo the resonant displacements of the jth mode is the summation of the kinetic energy and the potential energy of jth mode as (Tina 2007 a,b)

$$W_{\mathrm{j,r}} = \frac{1}{2}\dot{\boldsymbol{X}}_{\mathrm{j,r}}^{\mathrm{T}}(t)\boldsymbol{M}\dot{\boldsymbol{X}}_{\mathrm{j,r}}(t) + \frac{1}{2}\boldsymbol{X}_{\mathrm{j,r}}^T(t)\boldsymbol{K}\boldsymbol{X}_{\mathrm{j,r}}(t) \quad (20)$$

in which $\boldsymbol{X}_{\mathrm{j,r}}(\mathrm{t})$ and $\dot{\boldsymbol{X}}_{\mathrm{j,r}}(t)$ denote the resonant displacement vector and the resonant velocity vector of the jth mode, respectively, and they are equal to $\varphi_j q_{j,\mathrm{r}}(t)$ and $\varphi_j\dot{q}_{j,\mathrm{r}}(t)$, respectively, i.e.,

$$W_{j,\mathrm{r}} = \frac{1}{2}\dot{q}_{j,r}(t)\varphi_j^T\mathbf{M}\varphi_j\dot{q}_{j,\mathrm{r}}(t) + \frac{1}{2}q_{j,\mathrm{r}}(t)\varphi_j^T\mathbf{K}\varphi_j q_{j,r}(t) + \frac{1}{2}\dot{q}_{j,\mathrm{r}}(t) + \frac{1}{2}\omega^2 q_{j,\mathrm{r}}^2(t) \tag{21}$$

The expectation of the work done $W_{\mathrm{j,r}}$ is

$$W_{j,\mathrm{r,m}} = \frac{1}{2}E[\dot{q}_{j,\mathrm{r}}^2 + \omega_j^2 q_{j,\mathrm{r}}^2] = \frac{1}{2}\sigma_{j,\mathrm{r,v}}^2 + \frac{1}{2}\omega_j^2\sigma_{j,\mathrm{r}}^2 \tag{22}$$

where $\sigma^2_{\mathrm{j,r}}$ is variance of the jth-mode displacement and $\sigma^2_{j,\mathrm{r,v}}$ is the variance of the jth-mode velocity, as

$$\sigma_{j,\mathrm{r}}^2 = \int_{-\infty}^{+\infty} H_{j,\mathrm{r}}(\omega)\varphi_j^T\mathbf{L}\mathbf{S}_{\mathrm{PP}}(\omega)\mathbf{L}^T\varphi_j H_{j,\mathrm{r}}{}^*(\omega)d\omega \tag{23}$$

$$\sigma_{j,\mathrm{r,v}}^2 = \int_{-\infty}^{+\infty} \omega^2 H_{j,\mathrm{r}}(\omega)\varphi_j^T\mathbf{L}\mathbf{S}_{\mathrm{PP}}(\omega)\mathbf{L}^T\varphi_j H_{j,\mathrm{r}}{}^*(\omega)d\omega \tag{24}$$

The total energy of the resonant responses is the summation of energy expectations of the selected modes, i.e.,

$$W_{\mathrm{r,m}} = \sum_{j=1}^{K} W_{j,\mathrm{r,m}} \tag{25}$$

where K is the number of selected modes, for example the first 100 modes or the first 300 modes. Then the jth mode energy participation coefficient of resonant response is defined conveniently as follows

$$\lambda_{j,\mathrm{r}} = \frac{W_{j,\mathrm{r,m}}}{W_{\mathrm{r,m}}} \tag{26}$$

The mode participation factors of resonant response of selected modes are sorted in descending order and they are added together. The precision of the displacement of resonant response is controlled by a predefined minimum value of the mode participation coefficient of resonant response and the cumulative coefficient. The predefined minimum value of the cumulative factors for this study is 95%.

4. Wind-induced response of roof of BJNS

Based on the wind pressure time histories obtained from the wind tunnel test of the full-scale structure of the Beijing National Stadium, the displacement responses under the mean wind and fluctuating wind are computed. The controlling results, for wind azimuth 20 degree (Fig. 3), will be presented. The displacement responses under mean wind loads are given first in Fig.7. The background and resonant responses are investigated in the following sub-sections. Finally, the maximal and minimal displacement responses are presented for designer to estimate the safety of the structure.

4.1 Background response

4.1.1 Mode energy participation factors

The first 100-mode energy participation factors and the first 500-mode cumulative coefficients of

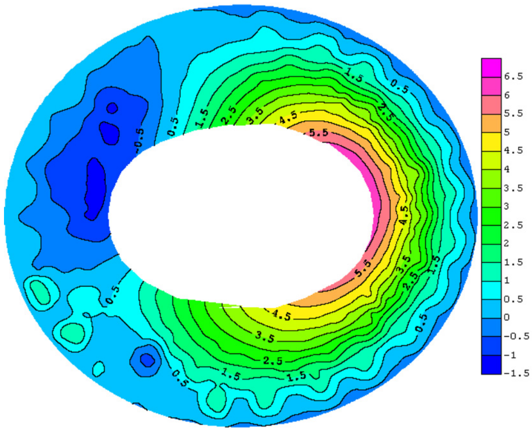

Fig. 7 Displacement under mean wind (mm)

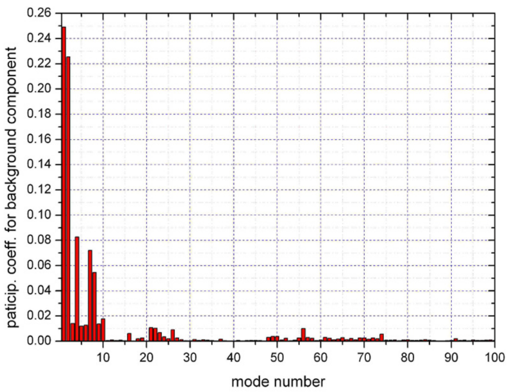

Fig. 8 Mode coefficients for background component

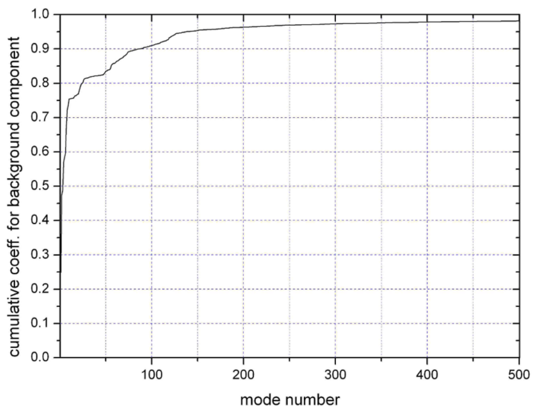

Fig. 9 Mode cumulative coefficients of first 500 modes

background response are shown in Figs. 8 and 9, respectively. It can be seen that the 1st, 2nd, 4th, 7th and 8th modes are the first 5 modes of ranked by their contributions to the responses and that the first 150-mode cumulative energy coefficient for the background component is greater than 95%. Furthermore, if the mode energy participation factors of the first 500 modes are sorted decreasingly, the first 55-mode cumulative energy coefficient is greater than 95%. These 55 modes are considered as the dominant modes of the background component and they are selected from Fig. 8.

4.1.2 Background response

The peak responses of the background component, shown in Fig. 10, are obtained from response from these 55 modes using complete quadratic combination procedure by letting the peak factor be 3.3, as the modal coupling effects among the dominant modes are always equal to unity as discussed in Eq.(12). Detailed analysis shows the inside edge vibrates freely and its response is dominated by the lower modes; the outside edge is supported on 24 steel columns and many higher modes are required to calculate the background responses accurately. However, the responses at the inside edge receive much more attention since the background responses at the outside edge is

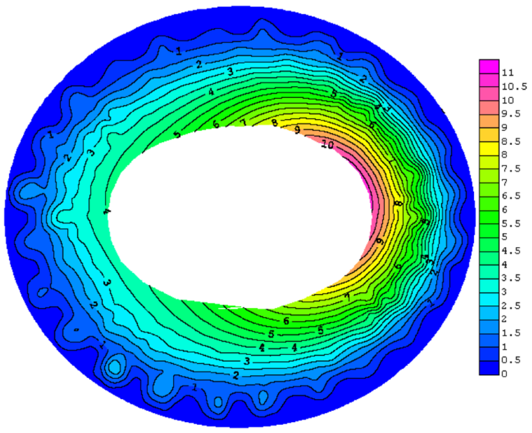

Fig. 10 Peak displacement responses for background component using CQC procedure (mm)

much smaller than those at the inside edge. Therefore the relative errors of responses at the outside edge can be neglected.

4.2 Resonant response

4.2.1 Mode energy participation factors

The first 50-mode energy participation factors of the resonant responses calculated by Eq.(26) are shown in Fig. 11 and the cumulative coefficients are shown in Fig. 12. It is indicated that the first 10 modes are very significant compared with other modes and that the cumulative coefficient of the first 25 modes is greater than 95%. If the mode energy participation factors are sorted decreasingly, the cumulative coefficient of the first 9 modes is greater than 95%. These 9 modes are called the dominant modes of the resonant responses.

4.2.2 Resonant Responses

The resonant responses can be formed by superimposing the 9 dominant modes using either the

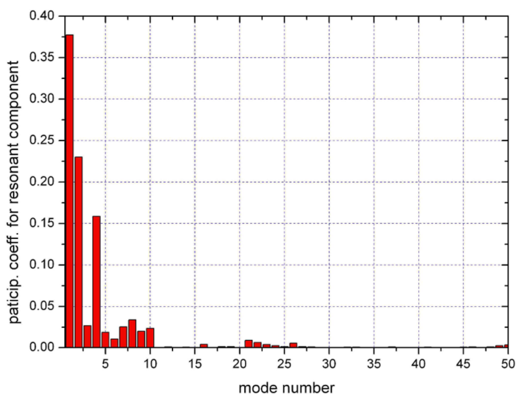

Fig. 11 First 50-mode energy factors of resonant response

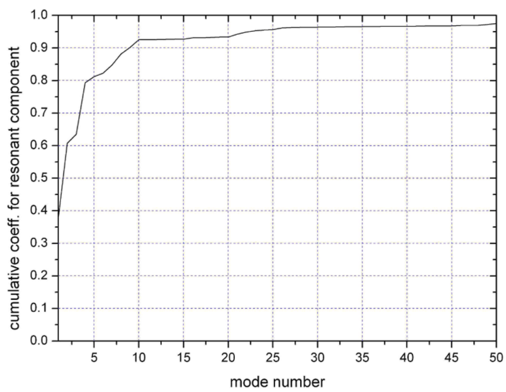

Fig. 12 Cumulative factors of resonant response

CQC procedure or the SRSS procedure. The peak resonant responses of these two cases are approximately identical and one of them, the SRSS result, is presented in Fig. 13, where the peak factors are also 3.3. This means that the coupling effect among the selected modes is negligible, which can also be inferred from that the modal spectral density around the modal frequency exhibits the flatness characteristic and that peak of the modal response is highly narrow.

4.3 Components combination

In Eq.(5), the fluctuating responses include three parts, i.e., the background component, the resonant component and the coupling item. For an example, Fig. 15 manifests the power spectra of the 1st modal responses, in which the resonant response is separated far from the background response and the coupling factors, defined in Eq.(10), between the two components is 1.9%. Further studies show the coupling item between the two components of any dominant mode is all less than 2%. Therefore the coupling effects between the two components are ignored in this study. The background responses shown in Fig. 10 and the resonant responses shown in Fig. 14 are then combined into the fluctuating responses, Fig. 16.

For roof structures, two combinations of the mean responses and the fluctuating responses, i.e., the summation and minus of the mean responses and the peak responses under fluctuating wind, are

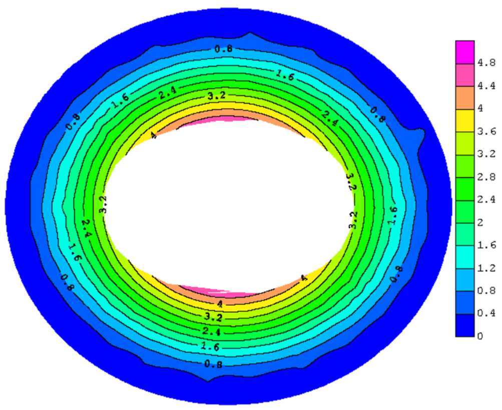

Fig. 13 Peak displacement of resonant response (mm)

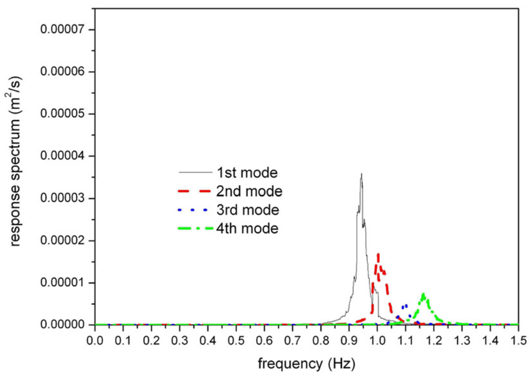

Fig 14 Response spectrum of resonant componen

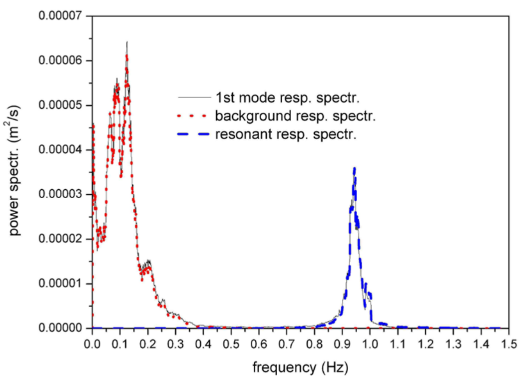

Fig. 15 1st mode response spectrum

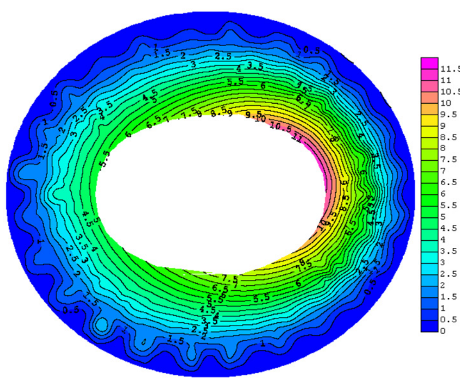

Fig 16 Peak displacement of fluctuating responses (mm)

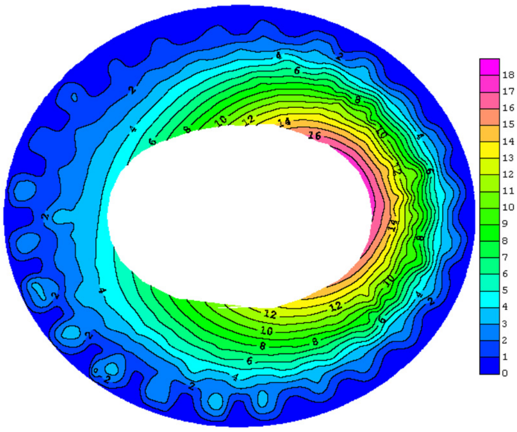

Fig. 17 Maximum response of BJNS roof (mm)

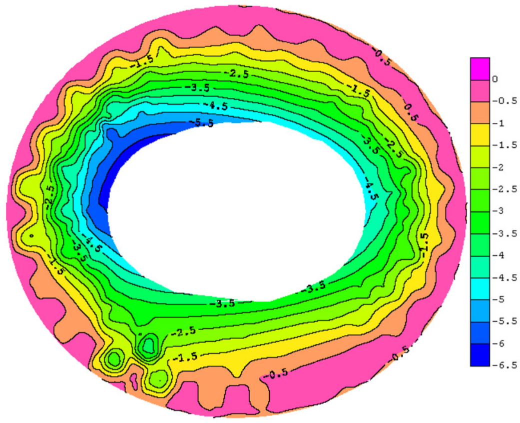

Fig. 18 Minimum response of BJNS roof (mm)

important for designing. Both of them (Figs. 17 and 18) are presented to the designer.

5. Conclusions

The three components, mean response, background response and resonant response, of the wind-induced responses for the Beijing National Stadium are investigated in this paper. The mode energy participation factors are presented to identify the dominant modes of the background and resonant responses.

Since the Beijing National Stadium is a relative rigid structure, the wind-induced responses are small, while the magnitudes of the mean responses are almost identical to the fluctuating responses. The background responses are significant in the fluctuating responses. The background responses of the dominant modes are coupled strongly because of the closely spaced frequencies and the wide-band spectrums while the coupling effect of the resonant responses of the dominant modes can be ignored because the resonant peaks are all narrow. The prevailing frequency of wind load is far away from the fundamental frequency of the roof of the BJNS and the correlation between background response and resonant response can be ignored.

Acknowledgements

This research is supported by the National Natural Science Foundation of China under Grant No. 90815021, 50978025 and 51021140005.

References

Ashraf, A.M. and Gould, P.L. (1985), “On the resonant component of the response of single degree-Fig. 17 Maximum response of BJNS roof (mm) Fig. 18 Minimum response of BJNS roof (mm) of-freedom systems under wind loading”, *Eng. Struct.*, **7**(4), 280-292.

Clough, R.W. and Penzien, J. (2003), Dynamics of structures, 3rd Edition, Computers & Structures, Inc.

Davenport, A.G. (1995), "How can we simplify and generalize wind loads?" *J.Wind Eng. Ind. Aerod.*, **54-55**, 657-669.

Gu, J.M., Ma, Z.D. and Hulbert, G.M.(2000), "A new load-dependent Ritz vector method for structural dynamics analyses: quasi-static Ritz vectors, finite elements in analysis and design", **36**(3-4), 261-278.

Nour-Omid, B. and Clough, R.W. (1985), "Block lanczos method for dynamic analysis of structures", *Earthq. Eng. Struct. D.,* **13**(2), 271-275.

Tian, Y.J., Yang, Q.S. (2007a), "Gust factors for large-span roof of the National Stadium", *Jianzhu Jiegou Xuebao, J.Build.Struct*., **28**(2), 26-31.

Tian, Y.J. and Yang, Q.S. (2007b), "Mode energy participation factors for fluctuating wind-induced response of large-span roof structure", *Zhendong Gongcheng Xuebao, J. Vib. Eng.*, **20**(3), 219-223.

Tian, Y.J. and Yang, Q.S. (2009), "Wind-induced responses of cantilevered steel roof of Olympic park tennis center stadium", *Jianzhu Jiegou Xuebao, J.Build. Struct.*, **30**(3),126-133.

Wilson, E.L., Yuan, M.W. and Dickens, J.M. (1982), "Dynamic analysis by direct superposition of Ritz vectors", *Earthq. Eng. Struct. D.*, **10**(6), 813-821.

Wu, Y., Zhang, J.S., Chen, B. and Shen, S.Z. (2007), "Identification of the dominant vibration modes of single-layer reticulated shells under wind action", *Int. J.Space Struct.*, **22**(2), 123-132.

CC